Designing low thermal conductivity of RuO2 for thermoelectric applications

Denis Music, Oliver Kremer, Gilles Pernot, Jochen M Schneider

Designing low thermal conductivity of RuO_2 for thermoelectric applications

Denis Music,[1,a)] Oliver Kremer,[1] Gilles Pernot,[2] and Jochen M. Schneider[1]
[1]*Materials Chemistry, RWTH Aachen University, Kopernikusstr. 10, 52074 Aachen, Germany*
[2]*University of Bordeaux, LOMA, CNRS UMR 5798, 33405 Talence, France*

We have applied Umklapp phonon-phonon and phonon-defect scattering to calculate the thermal conductivity of unalloyed as well as Fe- and La-alloyed RuO_2 ($P4_2/mnm$). These models are computationally efficient and parameter free as they are supported by density functional theory. We predict an order of magnitude drop in the thermal conductivity upon alloying, which is beneficial for thermoelectric applications as it increases the figure of merit. Thermal conductivity data obtained by thermoreflectance on magnetron sputtered thin films are consistent with the calculations. The here employed research strategy may also be beneficial for designing phases that require manipulation of entangled properties.

Efforts have been dedicated to investigate solids with desired thermal properties.[1,2] One such property of interest is thermal conductivity. In thermoelectric devices[3,4] and wear-resistive coatings,[5,6] a low thermal conductivity is required to increase the figure of merit and protect the tool, respectively, while in nanoelectronics and optoelectronics[1,7] heat needs to be promptly removed to prevent damage to the functional layers, thus large thermal conductivity is required. As the thermal conductivity is governed by transport of both charge carriers and phonons as well as their interplay with micro- and nano-structural features,[1,3,4] it is challenging to obtain predictive data from theoretical modeling. Especially in thermoelectric devices, it is central to decouple phonons from charge carriers to maximize the figure of merit.[3,4]

RuO_2 (space group $P4_2/mnm$, prototype rutile) is an appealing candidate for applications in thermoelectric devices owing to its surprisingly large electrical conductivity of $2.5 \times 10^6\ \Omega^1\ m^{-1}$, which is peculiar for oxides, and large thermal and chemical stability,[8] and hence it is used in microelectrical devices. Single-crystalline RuO_2 exhibits a very large thermal conductivity of $50\ W\ m^{-1}\ K^{-1}$,[9] which is consistent with electrical conductors such as Cr and Pt.[10] However, as the grain size is reduced, both phonon and electron scattering reduce the thermal conductivity. For 29 nm grains, a thermal conductivity of $19\ W\ m^{-1}\ K^{-1}$ was reported.[11] Further reduction of the thermal conductivity to $1\ W\ m^{-1}\ K^{-1}$ can be achieved by dilute alloying with La.[11] All these data were obtained at room temperature. This enormously large 50-fold reduction not only opens up possibilities for thermoelectric applications but it also enables other uses of this oxide such as high-power transistors and nano-assemblies with mechanical contacts, if this modulation can be understood and then further exploited.

In this work, we apply the so-called Slack model[12] and classical kinetic theory of phonon scattering to explain the difference in the thermal conductivity of unalloyed RuO_2 and La-alloyed RuO_2. We then predict the thermal conductivity of Fe-alloyed RuO_2 and validate this by thermoreflectance measurements on magnetron sputtered thin films. This strategy is efficient to design solids with desired thermal properties such as thermoelectrics where low thermal conductivity is required.

Within the Slack model,[12] the thermal conductivity (κ) can be obtained as follows:

$$\kappa = A\frac{M\theta_a^3\delta n^{1/3}}{\gamma^2 T}, \tag{1}$$

where A is a constant which can be determined as

$$A = \frac{2.43 \times 10^{-6}}{1 - 0.514\gamma^{-1} + 0.228\gamma^{-2}}, \tag{2}$$

with γ being the acoustic mode Grüneisen parameter.[13,14] M in Eq. (1) is the average atomic mass and θ_a is the Debye temperature of acoustic phonons calculated as

$$\theta_a = \theta n^{-1/3}. \tag{3}$$

Further parameters used above, such δ^3, n, and T designate the volume per atom, number of atoms in the cell, and absolute temperature, respectively.[12] The values for γ and θ_a can be obtained from elastic constants.[13,15] The elastic constants in this work were calculated using density functional theory,[16] as implemented in the Vienna *ab initio* simulation package (VASP) with projector augmented wave potentials,[17–19] which were parameterized within the generalized-gradient approximation by Perdew, Burke, and Ernzerhof.[20] The Blöchl corrections were applied for the total energy[21] and the integration in the Brillouin zone was carried out on converged Monkhorst-Pack k-points.[22] Full structural optimization was carried out for every system probed. The convergence criterion for the total energy was 0.01 meV within a 500 eV cut-off. The elastic constants were calculated by deforming the cells.[23–25]

As the Slack model was originally derived for dielectric phases describing the thermal processes close to θ_a, namely, Umklapp phonon-phonon scattering,[12] it is important to test

[a)]Author to whom correspondence should be addressed. Electronic mail: music@mch.rwth aachen.de

if the Slack model provides reasonable estimates of κ at room temperature for various systems. We have chosen typical thermoelectrics, such as Bi_2Te_3 and ZnO, as well as elemental Ge and Si as they are usually alloyed for thermoelectric applications.[3] Furthermore, we have also selected diamond since it possesses the largest θ_a value.[10] Figure 1 shows the comparison between the calculated and measured thermal conductivity. The measured data stem from the literatures.[10,26,27] It is worth noting that the data spread over three orders of magnitude. Even though the deviation between the measured and calculated data is within 21% to 88%, the right order of magnitude is obtained. Hence, the data obtained with the Slack model are consistent with the experimental data. It should also be observed that these data were obtained from elastic constants and no computationally demanding phonon or non-equilibrium molecular dynamics methods are used here.

One of the plausible reasons for the deviation between the measured and calculated data provided in Fig. 1 may be due to extrinsic effects such as structural defects. This becomes more pronounced when samples with smaller grain sizes are considered, e.g., those synthesized via sputtering and other non-equilibrium techniques. To account for these effects, we use a straightforward estimate based on classical kinetic theory of phonon scattering.[6] Thus, κ can be obtained as

$$\kappa = \frac{\lambda}{3} c_p v, \tag{4}$$

where λ is the phonon mean free path, which can be estimated from

$$\frac{1}{\lambda} = \frac{1}{\lambda_i} + \frac{1}{\lambda_{gs}} + \frac{1}{\lambda_a}, \tag{5}$$

where i, gs, and a designate intrinsic, grain size, and alloying effects, respectively. The average phonon velocity (v) can be computed from the elastic constants[15] and the specific heat capacity (c_p) is more demanding to calculate. Here, we use the intrinsic κ data from the Slack model to obtain the product of c_p and λ_i [1]. The first term in Eq. (5) was obtained from Eq. (4) as follows. Based on Eq. (4), it is clear that the

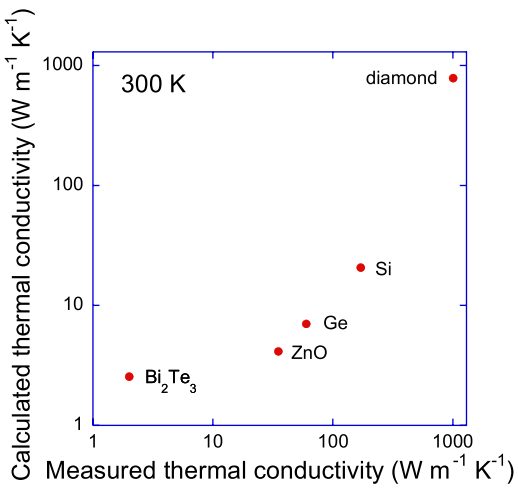

FIG. 1. Calculated and measured thermal conductivity for several dielectric phases. The Slack model was used.

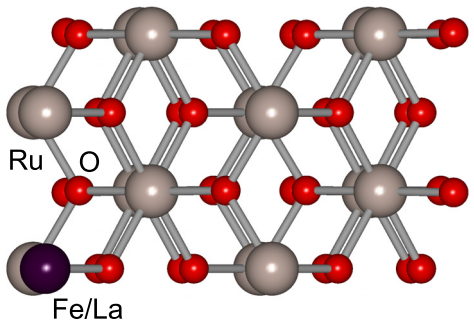

FIG. 2. RuO_2 ($P4_2/mnm$) alloyed with Fe or La.

thermal conductivity and mean free path are proportional. One of the proportionality constants is the average sound velocity, which was obtained from the elastic constants[15] and the other, namely, the specific heat capacity, was fitted from the Slack data for the unalloyed RuO_2, which is then assumed constant. For unalloyed RuO_2, no further corrections of the Slack model values in Eq. (5) were made as RuO_2 grows in the form of single-crystalline rods perpendicular to the substrate,[28–31] which is exactly the same direction the thermal conductivity was measured, see below. The second term in Eq. (5) was estimated based on a basic grain size consideration inspired by the Thornton structure zone model.[32] We assume that the mean free path is equal to the grain size, which we estimate to be $20 - 0.5*(T_h/c)$ in nm, where T_h is the homologous temperature (synthesis temperature divided by the melting point) and c is the alloying content. These constants (20 nm and 0.5 nm) were obtained by fitting the grain size data for Cu alloyed with Nb,[33] ZnO alloyed with Mg,[34] and γ-Al_2O_3 alloyed with Si.[35] The grain size data obtained here for alloyed RuO_2 are consistent with our direct observations.[11,36] The third term in Eq. (5) was obtained using the classical kinetic theory for scattering and hard sphere approximation,[6] where the cross-section was estimated from the size of the alloying elements. Both the Slack model and the classical kinetic theory are then applied for unalloyed RuO_2 and La-alloyed RuO_2. The rutile $2 \times 2 \times 2$ supercell containing 48 atoms, as treated in VASP, can be seen in Fig. 2. One Ru atom was replaced with La, resulting in the alloying content of 2.1 at. %. All elastic constants are provided in Table I. The bulk modulus data for unalloyed RuO_2 are consistent with the literature.[37] No literature data are available for the alloyed RuO_2.

Figure 3 contains the calculated and measured data for unalloyed RuO_2 and La-alloyed RuO_2. The measured data stem from the literature.[11] The experimentally obtained grain size was used. The calculated thermal conductivity decreases from 11.0 to 4.0 W m^{-1} K^{-1}, which is approximately a threefold drop. Even though the experimental decrease is approximately 20-fold, both calculated and measured values indicate an order of magnitude decrease thereby achieving consistency. Possible improvements of the calculated values may be obtained by including the electronic contributions to κ. As there is a substantial competition between majority and minority charge carriers in RuO_2[30] and the relaxation times are challenging to estimate using density functional theory, we do not include such effects. It is clear that the electronic effects would improve the agreement as La-alloyed RuO_2

TABLE I. Calculated bulk modulus (B) and elastic constants (C_{11}, C_{12}, C_{13}, C_{33}, C_{44}, and C_{66}) for RuO_2 as well as RuO_2 alloyed with La and Fe.

	B (GPa)	C_{11} (GPa)	C_{12} (GPa)	C_{13} (GPa)	C_{33} (GPa)	C_{44} (GPa)	C_{66} (GPa)
RuO_2[a]	265	324	247	170	553	147	239
RuO_2[b]	270 297	…	…	…	…	…	…
RuO_2 La[a]	249	301	228	162	524	130	217
RuO_2 Fe[a]	264	325	242	204	532	165	231

[a]This work.
[b]Reference 37.

possesses a twofold lower electrical conductivity than unalloyed RuO_2.[11] Based on the electrical conductivity of unalloyed RuO_2 and La-alloyed RuO_2[11] and the Wiedemann-Franz law with the Lorenz constant of 2.44×10^{-8} W Ω K^{-2},[38] the electronic contribution to the thermal conductivity can be estimated to be 16 and 6 W m^{-1} K^{-1} for these oxides, respectively. The Wiedemann-Franz law is in part valid for Fermi gas in metals. Here, band structure and additional scattering effects are clearly important. Still, if any electronic contributions to the thermal conductivity were present, they would give rise to improve the agreement between the predicted and measured thermal conductivities for these oxides.

We predict the thermal conductivity of Fe-alloyed RuO_2 to be 9.3 W m^{-1} K^{-1}, as shown in Fig. 3. To critically appraise our phonon-phonon and phonon-defect scattering approach, we measure the thermal conductivity of magnetron sputtered Fe-alloyed RuO_2 thin films. They were deposited in a vacuum system with a base pressure of $\sim 5 \times 10^{-5}$ Pa using reactive magnetron sputtering with a power density of 5.1 and 3.8 W/cm^2 for Ru (DC) and Fe (pulsed DC, 100 kHz) targets, respectively. The Ru and Fe targets (purity 99.9%) were mounted on magnetrons with the substrate-to-source distance of 10 cm and the angle of 19° between the substrate and plasma source normal. Si(100) substrates were kept at ~400 °C during synthesis. A mixture of Ar (99.9999%) and O_2 (99.9995%) was used as a sputtering gas with a partial pressure of 0.6 and 0.3 Pa, respectively. This gas mixture was selected based on the previous work.[39,40] The Ru Fe O thin film composition was determined using x-ray photoelectron spectroscopy (XPS) in a JAMP-9500F system (JEOL) with a K_α Al x-ray source (energy 1486.6 eV) and a hemispherical electron energy analyzer with a pass energy of 20 eV. The structural analysis was conducted by x-ray diffraction in a Bruker AXS D8 Discover General Area Detection Diffraction System with Cu K_α radiation. A collimator with a diameter of 0.5 mm and an incidence angle of 15° was used. A current setting of 40 mA and a generator voltage of 40 kV were applied. The κ value was measured with the time-domain thermoreflectance.[41] Prior to κ measurements, the sample was coated with aluminum. The thermal conductivity was carried out by adjusting the experimental signal with a 3-dimensional heat transfer model.[42] The Fe-RuO_2 samples exhibit the rutile structure and the Fe content is 2.4 at. %. The measured and calculated κ values for Fe-alloyed RuO_2 are 11.3 and 9.3 W m^{-1} K^{-1}, respectively, which is a deviation of 17% (see Fig. 3). Due to complexity of transport processes and structural defects present in real samples, the prediction of transport properties relevant for thermoelectrics is in the best case within 30%,[43] which implies that our predictions are acceptable. Here, we predict the thermal conductivity using only the elastic constants, which are computationally less demanding than full phonon calculations, and apply these data in the Slack model corrected for additional extrinsic phonon scattering effects. The synergy of theory and experiment, with deviation of the predicted thermal conductivity of only 17% for Fe-alloyed RuO_2, may lead to valuable speed up in knowledge based screening for efficient thermoelectrics.

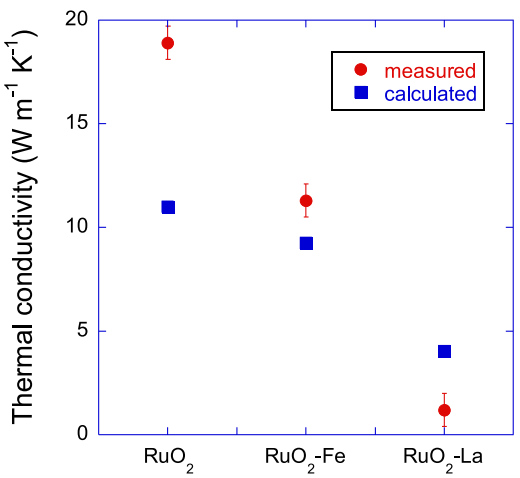

FIG. 3. Calculated and measured thermal conductivity for unalloyed RuO_2 as well as Fe and La alloyed RuO_2. The Slack model and classical kinetic theory were used.

Low thermal conductivity in a crystalline compound can in part be related to the bonding anharmonicity, which is related to the Grünesein parameter.[44] The lowest value of the thermal conductivity in this work is 1 W m^{-1} K^{-1} achieved for La alloyed RuO_2. The corresponding Grünesein parameter is 1.59. This is comparable to the value obtained for the thermoelectric $AgSbTe_2$ and PbTe compounds of 2.05 and 1.45, respectively.[45] These crystals exhibit the thermal conductivity of 0.68 and 2.4 W m^{-1} K^{-1}, respectively.[45] Hence, our data are consistent and the bonding anharmonicity plays an important role in this oxide as well. Other effects, such as extensive grain boundary phonon scattering, are also relevant as unalloyed RuO_2 and Fe-alloyed RuO_2 possess similar Grünesein parameters.

In conclusion, we applied the Slack model and classical kinetic theory to obtain the thermal conductivity of unalloyed and La-alloyed RuO_2. This is an efficient approach as no phonon calculations or non-equilibrium molecular dynamics are required, which would in turn be computationally rather demanding. This methodology was first tested in this work on standard thermoelectrics, such as Bi_2Te_3 and ZnO,

and then applied to RuO_2. Both the calculated and measured data consistently display an order of magnitude drop in the thermal conductivity upon alloying of RuO_2 with La. Furthermore, we predicted the thermal conductivity of Fe-alloyed RuO_2 to be 9.3 W m ^{1} K ^{1} and validated this by measuring the thermal conductivity of magnetron sputtered thin films. Disregarding electronic contribution to the thermal conductivity, the Slack model together with grain boundary scattering effects can be used to explain the modulation of the thermal conductivity of RuO_2 alloyed with La and Fe by a factor of 20. The obtained agreement of 17% not only indicates that this correlative theoretical and experimental research strategy is efficient to design solids with desired thermal properties but also identifies phonon-phonon and phonon-defect scattering as important mechanisms defining the transport properties in RuO_2 based compounds.

This work was supported by the Deutsche Forschungsgemeinschaft (DFG) within the project SCHN 735/24-1. The authors wish to thank Ali Shakouri from the Birck Nanotechnology Center at Purdue University for lending us his system for thermal properties characterization and Ida Z. Kozma from Menlo Systems GmbH for contribution in thermal conductivity measurements.

[1]D. G. Cahill, W. K. Ford, K. E. Goodson, G. D. Mahan, A. Majumdar, H. J. Maris, R. Merlin, and S. R. Phillpot, J. Appl. Phys. **93**, 793 (2003).
[2]T. Feng and X. Ruan, J. Nanomater. **2014**, 206370 (2014).
[3]G. J. Snyder and E. S. Toberer, Nat. Mater. **7**, 105 (2008).
[4]A. Bulusu and D. G. Walker, Superlattices Microstruct. **44**, 1 (2008).
[5]H. Holleck, J. Vac. Sci. Technol., A **4**, 2661 (1986).
[6]P. H. M. Bottger, E. Lewin, J. Patscheider, V. Shklover, D. G. Cahill, R. Ghisleni, and M. Sobiech, Thin Solid Films **549**, 232 (2013).
[7]G. Pernot, M. Stoffel, I. Savic, F. Pezzoli, P. Chen, G. Savelli, A. Jacquot, J. Schumann, U. Denker, I. Monch, C. Deneke, O. G. Schmidt, J. M. Rampnoux, S. Wang, M. Plissonnier, A. Rastelli, S. Dilhaire, and N. Mingo, Nat. Mater. **9**, 491 (2010).
[8]J. M. Lee, J. C. Shin, C. S. Hwang, H. J. Kim, and C. G. Suk, J. Vac. Sci. Technol., A **16**, 2768 (1998).
[9]D. Ferizovic´, L. K. Hussey, Y. S. Huang, and M. Munoz, Appl. Phys. Lett. **94**, 131913 (2009).
[10]C. Nordling and J. Osterman, *Physics Handbook for Science and Engineering* (Studentlitteratur, Lund, 1996).
[11]D. Music, F. H. U. Basse, L. Han, Devender, T. Borca Tasciuc, J. J. Gengler, A. A. Voevodin, G. Ramanath, and J. M. Schneider, Appl. Phys. Lett. **104**, 053903 (2014).
[12]G. A. Slack, J. Phys. Chem. Solids **34**, 321 (1973).
[13]B. D. Sanditov, S. B. Tsydypov, and D. S. Sanditov, Acoust. Phys. **53**, 594 (2007).
[14]W. Han Fu, C. Wei Guo, G. Yan Jun, and J. Hao, Chin. Phys. B **19**, 076501 (2010).
[15]Z. Sun, S. Li, R. Ahuja, and J. M. Schneider, Solid State Commun. **129**, 589 (2004).
[16]P. Hohenberg and W. Kohn, Phys. Rev. **136**, B864 (1964).
[17]G. Kresse and J. Hafner, Phys. Rev. B **48**, 13115 (1993).
[18]G. Kresse and J. Hafner, Phys. Rev. B **49**, 14251 (1994).
[19]G. Kresse and D. Joubert, Phys. Rev. B **59**, 1758 (1999).
[20]J. P. Perdew, K. Burke, and M. Ernzerhof, Phys. Rev. Lett. **77**, 3865 (1996).
[21]P. E. Blochl, Phys. Rev. B **50**, 17953 (1994).
[22]H. J. Monkhorst and J. D. Pack, Phys. Rev. B **13**, 5188 (1976).
[23]D. Music, T. Takahashi, L. Vitos, C. Asker, I. A. Abrikosov, and J. M. Schneider, Appl. Phys. Lett. **91**, 191904 (2007).
[24]L. Fast, J. M. Wills, B. Johansson, and O. Eriksson, Phys. Rev. B **51**, 17431 (1995).
[25]M. J. Mehl, J. E. Osburn, D. A. Papaconstantopoulos, and B. M. Klein, Phys. Rev. B **41**, 10311 (1990).
[26]Y. Zhang, R. J. Mehta, M. Belley, L. Han, G. Ramanath, and T. Borca Tasciuc, Appl. Phys. Lett. **100**, 193113 (2012).
[27]U. Ozgur, X. Gu, S. Chevtchenko, J. Spradlin, S. J. Cho, H. Morkoc¸, F. H. Pollak, H. O. Everitt, B. Nemeth, and J. E. Nause, J. Electron. Mater. **35**, 550 (2006).
[28]Y. T. Lin, C. Y. Chen, C. P. Hsiung, K. W. Cheng, and J. Y. Gan, Appl. Phys. Lett. **89**, 063123 (2006).
[29]M. H. Kim, J. M. Baik, S. J. L. H. Y. Shin, J. Lee, S. Yoon, G. D. Stucky, M. Moskovits, and A. M. Wodtke, Appl. Phys. Lett. **96**, 213108 (2010). D.
[30]Music, F. H. U. Basse, R. Haβdorf, and J. M. Schneider, J. Appl. Phys. **108**, 013707 (2010).
[31]D. Music, J. Breunung, S. Mr´az, and J. M. Schneider, Appl. Phys. Lett. **100**, 033108 (2012).
[32]J. A. Thornton, J. Vac. Sci. Technol. **11**, 666 (1974).
[33]S. Ozerinc¸, K. Tai, N. Q. Vo, P. Bellon, R. S. Averback, and W. P. King, Scr. Mater. **67**, 720 (2012).
[34]M. Salina, R. Ahmad, A. B. Suriani, and M. Rusop, Trans. Electr. Electron. Mater. **13**, 64 (2012).
[35]F. Nahif, D. Music, S. Mr´az, H. Bolvardi, L. Conrads, and J. M. Schneider, Surf. Coat. Technol. **235**, 250 (2013).
[36]D. Music, Y. T. Chen, R. W. Geyer, P. Bliem, and J. M. Schneider, Mater. Res. Express **1**, 045034 (2014).
[37]H. W. Hugosson, G. E. Grechnev, R. Ahuja, U. Helmersson, L. Sa, and O. Eriksson, Phys. Rev. B **66**, 174111 (2002).
[38]R. Franz and G. Wiedemann, Ann. Phys. **165**, 497 (1853).
[39]D. Music, F. H. U. Basse, and J. M. Schneider, Cryst. Growth Des. **10**, 4531 (2010).
[40]D. Music, N. A. Zumdick, B. Hallstedt, and J. M. Schneider, J. Appl. Phys. **110**, 054317 (2011).
[41]S. Dilhaire, G. Pernot, G. Calbris, J. M. Rampnoux, and S. Grauby, J. Appl. Phys. **110**, 114314 (2011).
[42]D. G. Cahill, Rev. Sci. Instrum. **75**, 5119 (2004).
[43]J. P. Heremans, B. Wiendlocha, and A. M. Chamoire, Energy Environ. Sci. **5**, 5510 (2012).
[44]L. D. Zhao, S. H. Lo, Y. Zhang, H. Sun, G. Tan, C. Uher, C. Wolverton, V. P. Dravid, and M. G. Kanatzidis, Nature **508**, 373 (2014).
[45]D. T. Morelli, V. Jovovic, and J. P. Heremans, Phys. Rev. Lett. **101**, 035901 (2008).